

Conceptualizing a Real-time Remote Cardiac Health Monitoring System

Alex Page

Dept. of Electrical and Computer Engineering, University of Rochester

Moeen Hassanali

Dept. of Electrical and Computer Engineering, University of Rochester

Tolga Soyata

Dept. of Electrical and Computer Engineering, University of Rochester

Mehmet K. Aktas

University of Rochester Medical Center, Department of Cardiology

Burak Kantarci

Department of Electrical and Computer Engineering, Clarkson University

Silvana Andreescu

Department of Bio-Chemistry, Clarkson University

ABSTRACT

In today's technology, even leading medical institutions diagnose their cardiac patients through ECG recordings obtained at healthcare organizations (HCO), which are costly to obtain and may miss significant clinically-relevant information. Existing long-term patient monitoring systems (e.g., Holter monitors) provide limited information about the evolution of deadly cardiac conditions and lack interactivity in case there is a sudden degradation in the patient's health condition. A standardized and scalable system does not currently exist to monitor an expanding set of patient vitals that a doctor can prescribe to monitor. The design of such a system will translate to significant healthcare savings as well as drastic improvements in diagnostic accuracy. In this chapter, we will propose a concept system for real-time remote cardiac health monitoring, based on available and emerging technologies today. We will analyze the details of such a system from acquisition to visualization of medical data.

Keywords: *e-Health, Tele-medicine, Remote health monitoring, privacy-preserving health monitoring.*

INTRODUCTION

Conventional tests to assess the risk of cardiovascular diseases (CVD) involve clinical history, physical examination and electrocardiogram (ECG), which are highly observational and relatively insensitive (Petr, et al., 2014; Prasad, et al., 2013; Saul, Schwartz, Ackerman, & Triedman, 2014; Vatta, 2009). Although the pathology of CVD starts at earlier stages than it is observable by conventional methodologies, there are no clinical tests that can detect the onset and progression of CVD. Continuous disease monitoring at a healthcare organization (HCO) is difficult as most tests rely on extensive hospital based procedures, and results can vary (Ndumele, Baer, Shaykevich, Lipsitz, & Hicks, 2012; Loon, et al., 2011; Kobza, et al., 2014; Juntilla, et al., 2014). Long-term real-time monitoring of clinically-relevant cardiac biomarkers remotely (e.g. at the patient's house) could provide invaluable diagnostic information, while eliminating the need to administer such tests at the HCO could translate to substantial cost savings.

Currently, there are no suitable methods to assess and predict the risk of CVD and chronic heart failure in real time to enable effective therapeutic intervention (Lin, Zhang, & Zhang, 2013; Jiao, et al., 2014; Gonzales, White, & Safranek, 2014). Mechanisms that are involved in the development of CVD are complex and involve a variety of interrelated processes including changes in blood cholesterol, lipid metabolism, inflammation and oxidative stress. Pathological role of reactive oxygen species (ROS) in the development of CVD, especially in conditions related to cardiac ischemia and chronic heart failure is well studied (Nojiri, et al., 2006; Otani, 2004; Searles, 2002; Singh, 1995; Tsutsui, 2001). Among ROS species, superoxide radicals and nitric oxide (NO) have both been identified as important parameters in the pathophysiological alterations in myocardial and vascular function (Kundu, 2012; Salamifar & Lai, 2013). Other studies have related cardiac proteins including cardiac troponins (cTn), myoglobin (MYO), b-type natriuretic peptide (BNP) and C-reactive protein (CRP) with the onset of cardiac infarction (Wojciechowska, et al., 2014).

The proposed system in Figure 1 will enable physicians to monitor patients and have automatic alarm providing feedback on patient long-term health status. This monitoring can be continuous in patients with high risk for life-threatening events, or periodic with a recording frequency depending on disease severity. This system is capable of monitoring ECG-related parameters using commercially available ECG patches, as well as multiple other aforementioned bio-markers of a patient via custom bio-sensors in real-time. Sensory recordings of the patient will be transmitted from the patient's house (or any remote location) to the datacenter of the HCO in real-time in a secure fashion using well established encryption mechanisms (NIST:FIPS-197, 2001). Combining ECG monitoring parameters with such biomarkers improves the utility of the monitoring system to far beyond what is currently achievable with ECG-only monitoring or single-biomarker monitoring (e.g., Glucose (Sensys Medical)). This technology will be disruptive because it has the potential to shift the paradigm of patient management in the US healthcare system.

While the comprehensive nature of this system substantially improves its diagnostic value, it introduces research challenges which this chapter aims to address. Visualization of such multi-dimensional data, encompassing ECG parameters and multiple bio-markers is not straightforward. Well known ECG-based visualization of a patient's cardiac operation has been in use for over a century (Fridericia, 1920), but provides limited information for a short operational interval. In this chapter, visualization mechanisms will be presented that allow the doctor to visualize ECG recording parameters over 24 hours.

The chapter will detail the design of a concept real-time remote health monitoring system as follows. Next section presents the state of the art in bio-medical sensing, particularly focusing on nanoparticle-based detection of biomarkers, use of electrochemical sensors for the detection of oxidative stress, label-free aptasensors for the detection of bio-molecular recognition process and the integration of field portable biosensors with wireless communication devices. This first section, which focuses mainly on the chemical aspects of the system in Figure 1, will be followed by design considerations for bio-

sensor circuit interface. A tamper-resistant sensing mechanism will be introduced along with the circuit interface which takes advantage of the chemical properties of the sensors. Third section will present an Internet-of-Things (IoT)-based sensory architecture, focusing on concentrator and cloudlet designs, as well as reliable and trustworthy sensing schemes. Communications standards, as well as inter-operability issues for the presented architecture will be elaborated on in the fourth section, followed by the last section presenting visualization components. Concluding remarks as well as a discussion of the open issues and future directions will be provided at the end of the chapter.

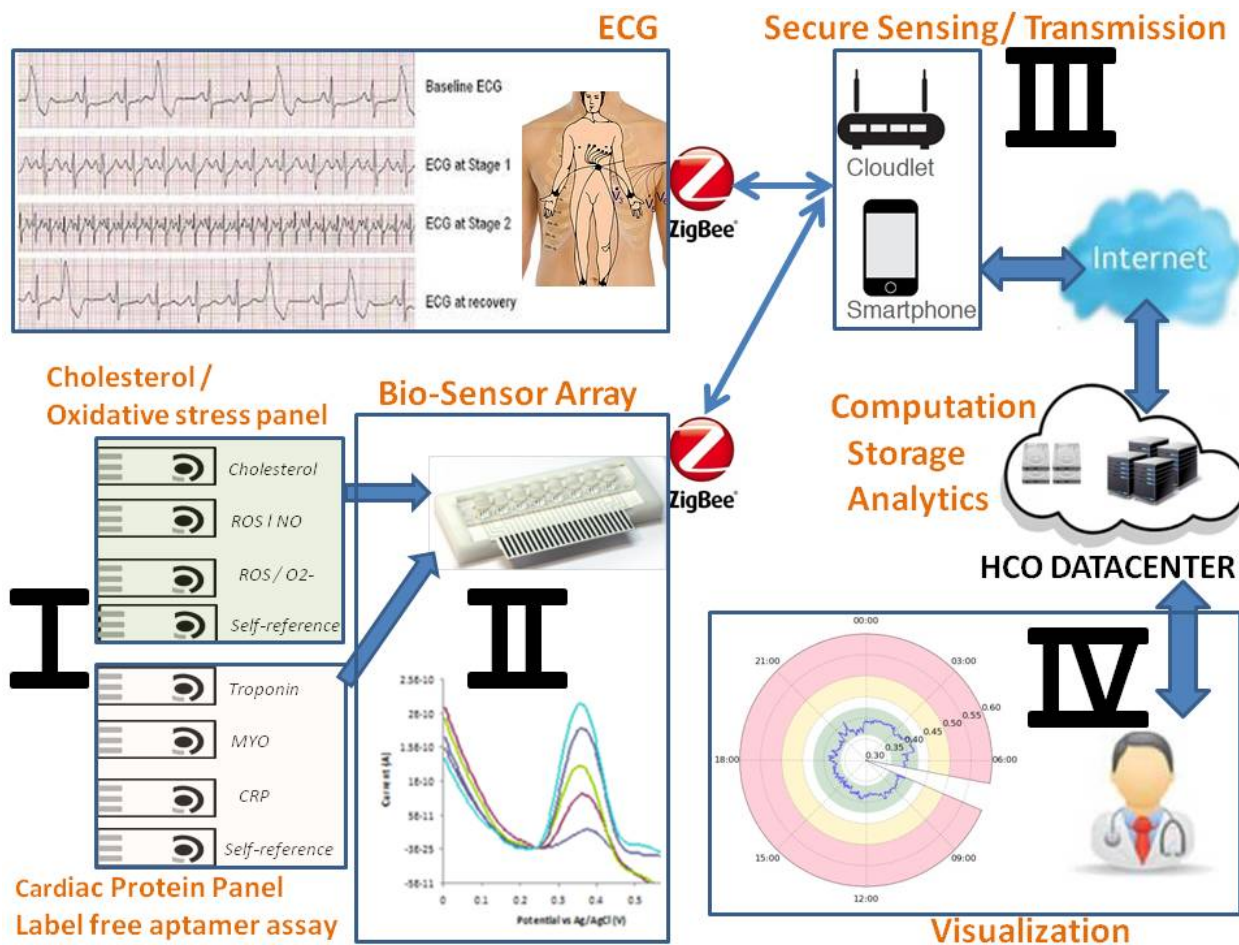


Figure 1: Proposed cardiac monitoring system: I) sensory acquisition, II) sensor interface, III) secure data transmission, IV) visualization and analytics.

BIO-MEDICAL SENSOR DESIGN

A comprehensive cardiac monitoring system requires the real-time detection of oxidative stress as well as the aforementioned cardiac proteins such as Troponin, MYO, and CRP as shown in **Figure 1** (denoted as "I"). For the nanoparticle based detection of clinically relevant biomarkers, Andreescu's laboratory has pioneered an inexpensive sensing technology based on redox active nanoparticle of cerium oxide (nanoceria) used as catalytic amplifiers (Ornatska, Sharpe, Andreescu, & Andreescu, 2011). This

technology is based on probing biomolecular interactions to determine clinically relevant biomarkers with high sensitivity and selectivity, enabling the detection of NO, superoxide radicals, H₂O₂, glucose, dopamine, glutamate and antioxidants (Sharpe, Frasco, Andreescu, & Andreescu, 2013) in biological fluids including plasma, cerebrospinal fluid, tissues and animals (Cortina-Puig, et al., 2010; Njagi, Ball, Best, Wallace, & Andreescu, 2010; Ozel, Ispas, Ganesana, Leiter, & Andreescu, 2014; Ganesana, Erlichman, & Andreescu, 2012). These designs take advantage of redox and surface functionality changes of nanoceria particles in the presence of redox compounds associated with biomolecular recognition events, including catalytic enzyme reactions and biomolecular recognition events (Hayat & Andreescu, 2013; Hayat A. , Andreescu, Bulbul, & Andreescu, 2014; Hayat, Bulbul, & Andreescu, 2014). In the presence of H₂O₂, the nanoceria enhances the catalytic oxidation of H₂O₂ (Ornatska, Sharpe, Andreescu, & Andreescu, 2011) leading to increased sensitivity for the detection of H₂O₂ as a model of ROS, and of substrates of oxidase enzymes that are enzymatically producing H₂O₂ (Babko & Volkova, 1954; Hayes, Yu, OKeefe, & Stoffer, 2002). These sensors have detected physiological levels of glucose, dopamine, glutamate and lactate in clinical samples using both colorimetric (Ornatska, Sharpe, Andreescu, & Andreescu, 2011) and electrochemical methods (Ornatska, Sharpe, Andreescu, & Andreescu, 2011; Ispas, Njagi, Cates, & Andreescu, 2008; Njagi, Ispas, & Andreescu, 2008).

We hypothesize that by measuring various biomarkers in parallel, correlating them to conventional ECG tests, and tracking their evolution, it is possible to quantitatively define a clinical cardiac risk profile that can be used in the prevention and personalized therapeutic intervention of cardiac diseases. Two custom multi-sensor arrays must be developed to assess the evolution of biomarkers related to different CVD mechanisms as shown in Figure 1. Cholesterol/oxidative stress panel includes Cholesterol(Ch), superoxide radicals (O₂⁻) and nitric oxide (NO), while the protein panel includes cTn, MYO and CRP, which have been associated with the onset of myocardial infarction. In (Alkasir, Ornatska, & Andreescu, 2012), Alkasir et al. developed portable sensors with colorimetric and electrochemical detection for monitoring clinical analytes including glucose (Ornatska, Sharpe, Andreescu, & Andreescu, 2011) glutamate, dopamine and antioxidants (Sharpe, Frasco, Andreescu, & Andreescu, 2013), and low-cost screen-printed sensors that are the basis of portable glucose monitoring devices (Alkasir, Ganesana, Won, Stanciu, & Andreescu, 2010; Istamboulie, Andreescu, Marty, & Noguier, 2007; Andreescu, Barthelmebs, & Marty, 2002; Andreescu, Magearu, Lougarre, Fournier, & Marty, 2001) and a multi-sensor array that allows field detection of multiple compounds (Sharpe, et al., 2014), where each sensor in the array contains a different signal responsive material that reacts with a target analyte (Hayat & Andreescu, 2013), as exemplified in Figure 2. Proposed system should expand on (Hayat & Andreescu, 2013) to monitor conformational changes of surface-confined aptamers towards biomarkers including MYO, CRP and BNP.

The proposed system in this chapter is based on the sensors developed in (Ornatska, Sharpe, Andreescu, & Andreescu, 2011; Hayat, Bulbul, & Andreescu, 2014; Ozel, Ispas, Ganesana, Leiter, & Andreescu, 2014). Figure 3 depicts a NO sensor voltammogram, in which the sensor responds to different voltage excitations (x axis) with a resulting current (y axis) at varying NO concentrations (different colors). Figure 3 could be thought of as being a 3D plot, with voltage (x), current (y), and concentration (z) axes. For sensing, voltage axis (x) is omitted by plotting concentration–current curves at a fixed voltage yielding the highest current (e.g., 0.35V for the NO sensor in Figure 3). The resulting 2D calibration curve contains all necessary information for optimum sensitivity.

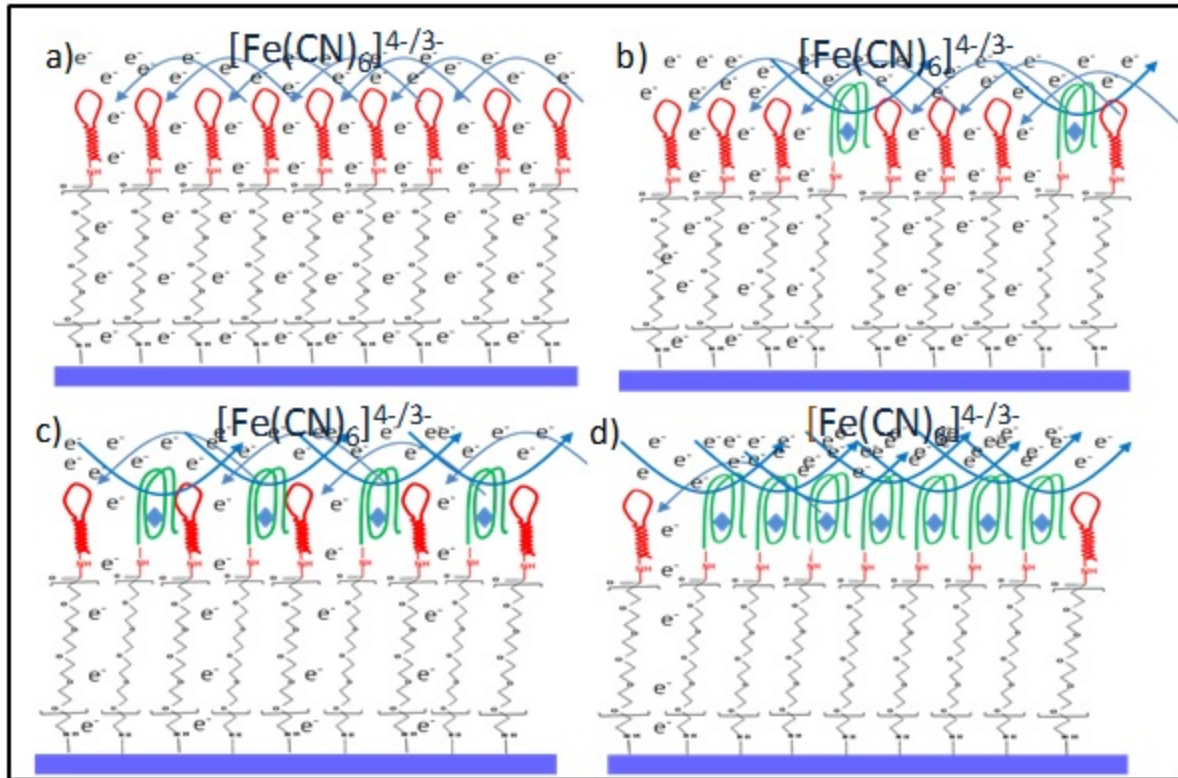


Figure 2: Label free detection of OTA based on conformational changes of surface confined aptamer-PEG macromolecular adducts showing sequential electrochemical detection steps.

To enable early detection and prevention, there is a need for a methodology that could quantify clinical changes related to the evolution of disease and transmit the information in real time to the health care provider for early intervention. In this aim, we suggest that, cardiac biomarkers, combined with ECG parameters will provide a comprehensive set of diagnosis data. The proposed sensor will consist of a series of electrodes, each designed to detect one specific biomarker. The probe can be multiplexed in order to quantify multiple cardiac biomarkers simultaneously. To draw fundamental biomedical information regarding the evolution of these biomarkers, this sensor data must be correlated with ECG recording from cardiac patients. This will allow individual profiling of a cardiac risk for monitoring the progression of cardiac disease and assess an individualized risk factor. The development of electrochemical microsensors, which have been successfully used in vitro and in vivo settings are documented in (Ganesana, Erlichman, & Andreescu, 2012; Njagi, Ball, Best, Wallace, & Andreescu, 2010).

This chapter proposes to integrate these sensors to measure comprehensively the oxidative/nitrosative profile, and correlate these data with cardiac protein biomarkers, and ECG. Our proposed testing of this technology is to study samples from cardiac patients in microliter blood samples and the assessment of the selectivity of these sensors for measurements in other matrices that are collected non-invasively including urine and saliva. This chapter focuses on two classes of biomarker signatures: (a) cholesterol and oxidative stress profile that involves time point measurements of the evolution of the

cholesterol system and oxidative stress, and (b) a protein biomarker panel to determine proteins that are predictive of myocardial infarction. The sensors can be fabricated on low cost disposable screen-printing (SPE) platforms. These two types of biomarker signatures will be detailed below.

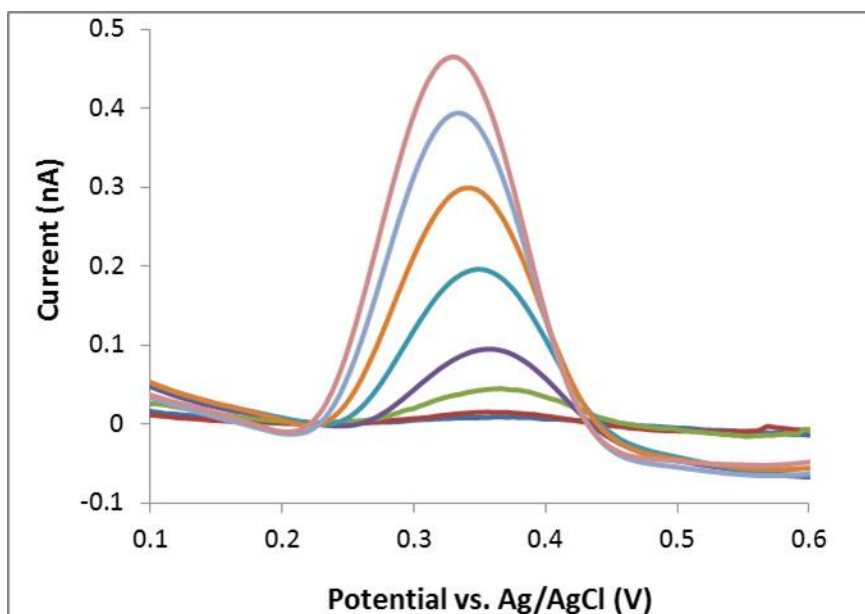


Figure 3: Electrochemical responses to various concentrations of NO using differential pulse voltammetry.

Cholesterol and Oxidative Stress Panel

First, we propose to integrate the recently developed sensor with nanoparticle amplification (Ornatska, Sharpe, Andreescu, & Andreescu, 2011) into an array system. The cholesterol sensor will utilize the enzyme cholesterol oxidase that will be stabilized on the SPE working electrode which will measure electrochemically the enzyme generated H_2O_2 at its oxidation potential of 0.5 V. Previously developed sensors based on this technology allow sensitive detection of physiological levels of glucose in human serum (Ornatska, Sharpe, Andreescu, & Andreescu, 2011). The superoxide sensor will use surface attached cytochrome c and will measure the reduction of cytochrome c by O_2^- as was reported in (Ganesana, Erlichman, & Andreescu, 2012). Cytochrome c must be immobilized on self-assembled monolayers of mixed thiols to facilitate direct electron transfer upon interaction with O_2^- (Winterbourn, 2008; Ge & Lisdat, 2002). For NO, we propose to use permselective membranes and electrodeposited Meldola Blue catalysts which we found to selectively interact with NO, thus enhancing sensitivity (Njagi, Ball, Best, Wallace, & Andreescu, 2010). NO must be quantified electrochemically at 0.9 V vs. Ag/AgCl. Readings will be repeated over time at different periods to provide a longitudinal monitoring profile of these species.

Protein Biomarker Sensors

We propose to design a sensor array with biomolecular recognition using aptamers which consists of four sensors: three to analyze a cardiac biomarker: cTn, MYO and CRP; and a control sensor for use in the

tamper-resistance scheme as will be explained later in this chapter. Aptamers for cardiac cTn, MYO and CRP are commercially available and will be used in our sensor design. Figure 4 highlights the general fabrication procedure and detection mechanism based on redox nanoparticles and aptamer chemistry as an example of sensor for Troponin (cTn). Aptamer functionalized screen-printed electrodes with both recognition and sensing functions must be used as active sensing components. As previously discovered, nanoceria particles can act as redox amplifiers in biorecognition assays and enhance catalytic and electrochemical signals allowing us to measure nM concentration of target analytes (Hayat & Andreescu, 2013). Binding of target functionalized nanoceria to aptamer modified electrodes after exposure to the target analyte will induce specific binding and conformational changes of the aptamer through a competitive mechanism, which will change the electrochemical properties of the bioelectrode in a concentration dependent manner.

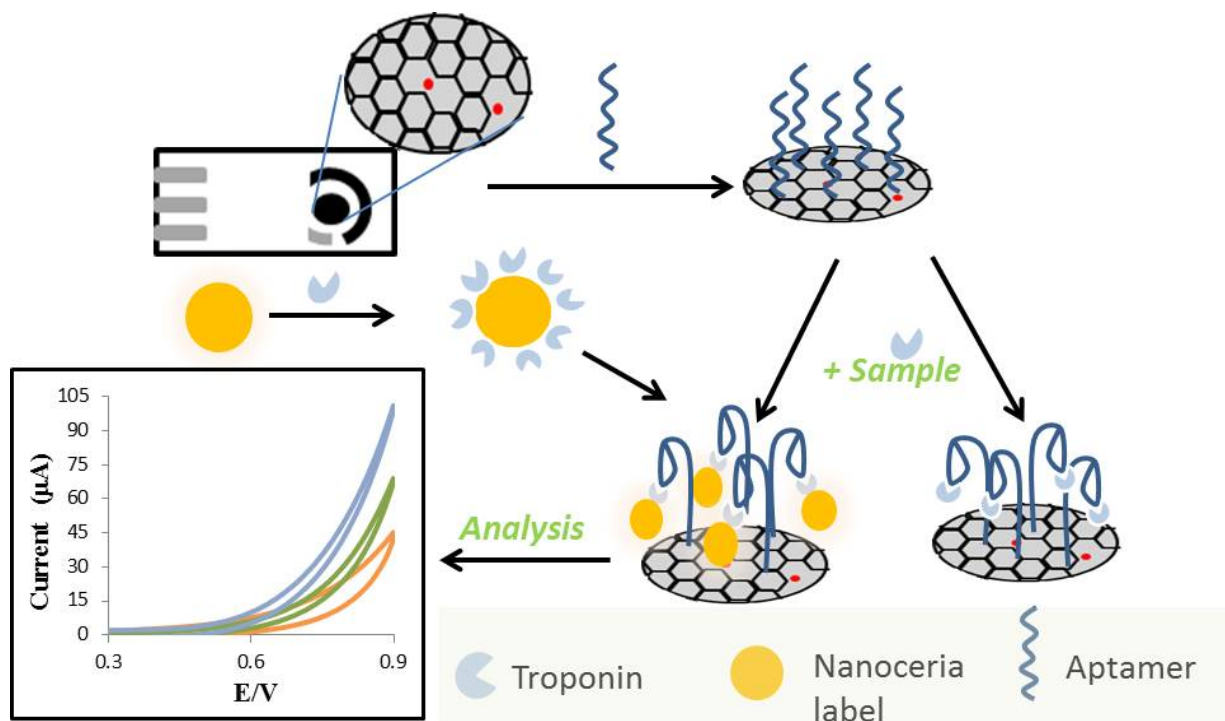


Figure 4: Aptamer biosensor fabrication using affinity recognition and redox active nanoceria particles as catalytic amplifiers.

We propose to evaluate the Redox behavior of aptamer binding by measuring the spectral and electrochemical properties of unmodified and modified bioelectrodes in the presence and absence of cardiac biomarkers using electrochemistry. Redox reactivity studies and the effect of surface coverage will be evaluated by electrochemical methods, cyclic voltammetry (CV) and electrochemical impedance spectroscopy (EIS). Biomodification of the nanoceria particles with cardiac specific aptamers is expected to increase the electron transfer resistance and induce a decrease in the voltammetric response of an electrode covered with biofunctionalized nanoceria, in a concentration-dependent manner. The effect of the amount of immobilized bioreceptors and biofunctionalized particles, the incubation time and specificity of binding, and the electrochemical parameters (e.g. electrolyte, potential) must be established

and optimized. Higher concentration of biomolecules and particle bioconjugates can potentially increase the signal, but they can also reduce the sensitivity and increase non-specific recognition. Long incubation time will enhance the signal but it will also increase analysis time and decrease sensitivity. Operational parameters including concentration of nanoparticles, incubation time and linearity range must be optimized. Tests for long-term stability upon storage of the biofunctionalized must also be performed using similar procedures. Conventional biochemical ELISA assays must be used for validation of the proposed sensor array. Protocols for optimum bioassay design that provides the highest biorecognition ability, stability and sensitivity must be determined. At the end of this task, we expect to have bioactive sensors with high affinity recognition and detection capability for cardiac biomarkers, and identifying the best sensor design for uses in real clinical samples.

BIO-SENSOR CIRCUIT INTERFACE

The circuit interface to the sensor array design that we proposed in the previous section is denoted as "II" in **Figure 1** and will be explained in detail in this section. **Figure 3** shows the response of an example NO sensor which has an optimum operating voltage of 0.35V. A calibration curve (i.e., concentration–current curve) is created such as the one shown in **Figure 5** for these optimum voltages. Therefore, the voltage axis is eliminated in the resulting calibration curve. While the measurement of the current response involves applying 0.35V to the sensor and performing a straightforward Analog-to-Digital (ADC) conversion on the current, our goal is to embed built-in security counter-measures directly into the sensor operation against sensor tampering. So, we will be proposing the design of the sensor interface circuitry with tamper-resistance as a top priority.

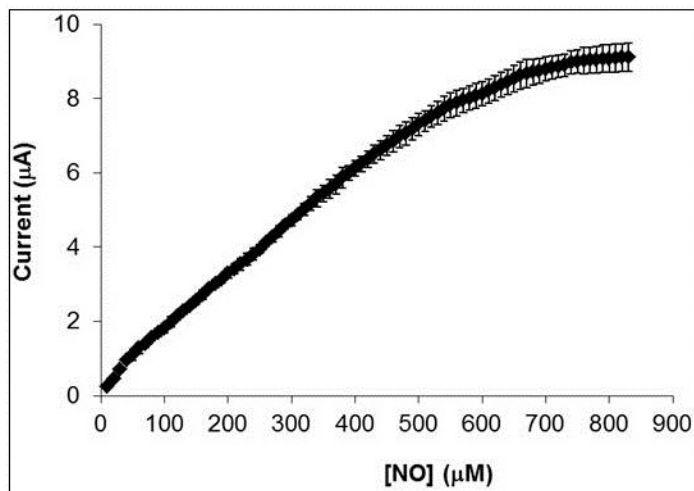


Figure 5: 2D Calibration curve of an NO sensor.

Low Power Sensor Circuit Interface

The primary goal of the sensor circuit design is measuring the sensor response by using the least amount of energy. We envision an inexpensive disposable sensor which operates from a standard CR2032 Lithium coin battery (CR2032) CR2032 has a 225mAh energy density @3V, corresponding to a

$0.225 \times 3 \times 3,600 = 2,790$ Joules energy storage capacity. Due to the very low bandwidth of the information that needs to be transmitted from the sensor to the concentrator, which aggregates data from multiple sensors, if we assume a duty cycle of 1% (i.e., 99% no transmission, and 1% burst transmission), average power consumption of the sensing circuitry is

$$P_{avg} = P_{sensor} + P_{uC} + P_{Zigbee} = (10\mu\text{A} \times 0.35\text{V} \times 8) + (150\mu\text{A} \times 3\text{V}) + (60\text{mW} \times 0.01) \approx 1.06\text{mW} \quad (1)$$

where P_{sensor} is the power consumption of each sensor circuit (total 8 sensors), P_{uC} is the power consumption of an 8 bit microcontroller which is sufficient for this operation with a built-in ADC, and P_{Zigbee} is the power consumption of Zigbee communication at the activity rate of 1%. This simple back-of-the-envelope calculation shows that, a CR2032 battery can sustain the sensor circuitry for $2,790 / (1.06 \times 10^{-3} \times 3,600) = 731$ hours which corresponds to almost a month. We do not envision the remote patient monitoring to be longer than this, so, this design with a CR2032 battery is sufficient. However, other techniques to reduce the power consumption via more sophisticated communication techniques, which can in turn be used for implementing higher security measures, are feasible and is left for future research.

Current going through the sensor can be measured by measuring the voltage drop on a sense resistor placed in series with the sensor (Hassanaliyagh, Soyata, Nadeau, & Sharma, 2014). Sense resistor voltage drop can either be directly fed into a an ADC or it has to be amplified prior to conversion, by using a *current sense amplifier*. If the voltage drop is too small, a sense amplifier must be used to bring the voltage drop within the range of the ADC. Figure 6 shows a simple circuit for sensing/amplifying the sensor current. The circuit portion encompassed in the dashed lines can be eliminated if signal amplification is not needed. This is the case when a high-valued sense resistor is used, resulting in a large voltage drop such as $\sim 1\text{V}$, which can be directly converted by the ADC within the microcontroller without loss of conversion accuracy.

A high valued sense resistor implies a high power consumption incurred by the sense resistor, thereby increasing the power burden of the sensing operation. On the contrary, a small sense resistor eliminates excessive power consumption due to the low voltage drop across it (e.g., 20-100 mV), albeit at a reduced accuracy of conversion (Gekakis, et al., 2015). For example, if only a 100 mV voltage drop is allowed across the sense resistor which is applied to a 12b ADC operating from a voltage references of $V_{ref} = 1.024\text{V}$, full range of 1.024 V means 12 bits of accuracy, while only an 7 or 8 bit accuracy can be achieved with a 100 mV sense voltage due to the 10x range reduction. Considering the 1 to 2 bit of built-in inaccuracy that is inherent in the design of the ADC itself, this only equates to an effective 6 bit overall conversion accuracy. The accuracy problem is exacerbated when even a lower voltage drop is allowed in the sense resistor, thereby making the use of a current sense amplifier necessary. However, this also introduces a power consumption that is incurred by the sense amplifier itself. From a practical standpoint, the measurement accuracy is always a much more important consideration than the small amount of incremental power consumption incurred by the sense amplifier. A vast array of commercially-available ultra-low power consumption sense amplifiers (e.g., (MAX4372)) make the use of an amplifier the most meaningful choice in such a system.

As we can see in Figure 3, for the best sensitivity of sensor current to NO concentration, the excitation voltage applied to the sensor must be approximately 350 mV. According to Figure 6, sensor voltage is the excitation voltage subtracted by the voltage drop on the sense resistor. For precise measurements, we would like to keep the sensor voltage fixed. As the sensor current changes, so does the

voltage drop on the sense resistor. We can achieve fixed sensor voltage goal by two means: 1) Using a small enough sense resistor so the variation of sense voltage is negligible compared to the applied excitation voltage, and 2) dynamically adjust the excitation voltage based on the measured voltage drop to keep the sensor voltage constant. In case of a fixed excitation voltage reference of 350 mV, in order to keep the sensor voltage within 5 % of the desired 350 mV voltage, a maximum voltage drop of 18 mV is allowed on the sense resistor in full scale. In order to use off-the-shelf ADCs with high resolution data conversion, a current sense amplifier with a gain of order of 100 is required to amplify the voltage drop. Choosing an appropriate amplifier in data conversion applications which meets the circuit voltage range, noise, and bandwidth specifications is a key factor. A complete guide for amplifying circuit design for interfacing to data converters can be found in (ADI-ReportADC, 2015). Since in our proposed battery based system, low power consumption and operation longevity are key parameters, excessive care must be taken when adding an extra component which increases the overall system power consumption. For example, MAX4372H (MAX4372) is a low cost, but reasonable precision current sense amplifier, demanding a supply current of 30 μA . If operated at 3 volts, it consumes 90 μW which almost adds 10% to the pre calculated average power consumption.

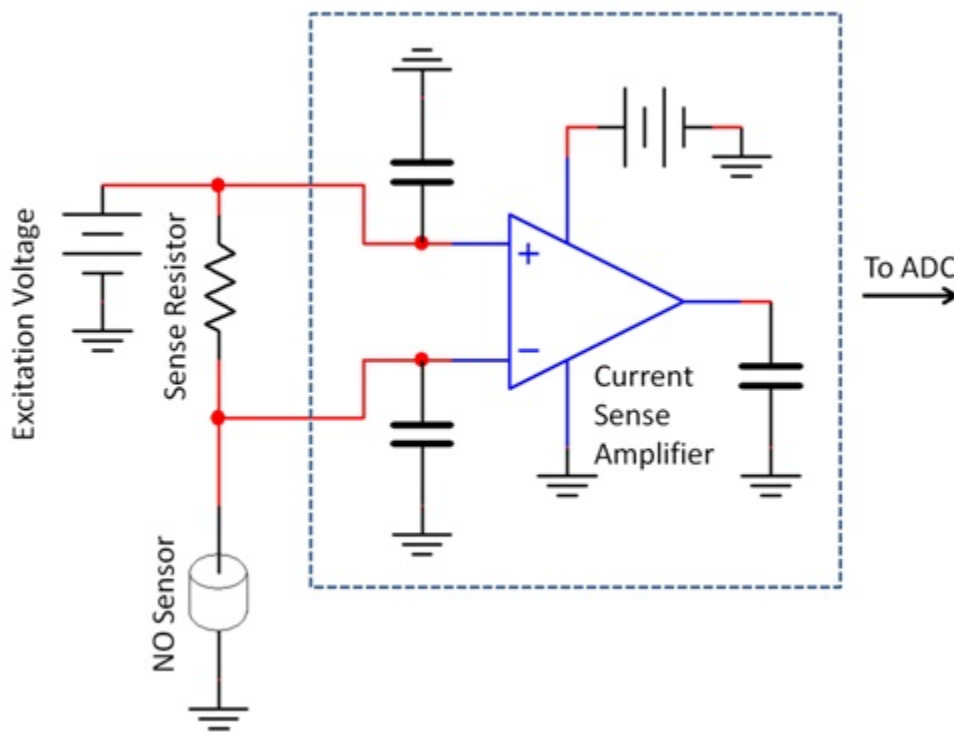


Figure 6: A simple sense and amplifying circuit for the NO sensor current readout. The circuit part included in dashed line can be eliminated when using an adjustable excitation voltage and highly enough sense resistor for direct measurement of the voltage drop.

In our proposed system, a programmable excitation voltage is a more desirable choice, as it provides the system with the flexibility of interrogating the sensors within an extended range of excitation

voltages, which will increase the system's security against possible sensor tampering, as will be explained shortly in our *Challenge-based Sensing* section. PIC16F1783 (PIC16F1783) which is an 8-bit low power microcontroller with an integrated ADC (Analog-to-Digital Converter) and DAC (Digital-to-Analog Converter), which completely suits our application. An internal 12 bit differential ADC with a programmable reference voltage can be used for direct measurement of the sense voltage. The integrated DAC in the microcontroller can be used to generate the variable excitation voltage.

Sense resistor value can easily be calculated according to the ADC full scale voltage and the NO sensor current. As we can see in Figure 3, at the excitation voltage 350 mV, maximum sensor current is approximately 0.45 nA. So if the ADC full scale voltage is 1024 mV, a sense resistor smaller than 2.28 M Ω should be used. However in order to keep sensor voltage at 360 mV, the applied excitation voltage has to vary in the range 350 mV - 1384 mV.

Incorporating Tamper-Resistance into the Sensor and Sensing Circuitry

To ensure tamper-resistance within the sensor array against different tampering scenarios, we propose two ideas during the sensing operation: 1) Through the addition of a fourth *blank* sensor, and 2) by interrogating the sensors at different multiple redundant voltages. Both of these scenarios imply redundant work to achieve sensing privacy. In the proposed medical data acquisition system, the benefits of privacy are clear and the additional power consumption incurred by these techniques through redundant sensing and redundant computations are more than justifiable. We will now explain our tamper-resistance ideas in detail below.

Control Sensor to Detect Relocation Tampering

The first idea is the addition of a fourth sensor (control sensor) to each sensor array, in addition to the three other sensors, each sensing a specific biomarker. We hypothesize that, the addition of this fourth sensor can facilitate the bio-identification of the patient that is being monitored. This will allow the detection of a simple placement of the sensor to *another person*. We define this as *relocation tampering*. Although this is the simplest form of tampering, its ability to fool the system is surprisingly high. This is a highly likely scenario when an involuntary (or even voluntary) placement of a sensor to another person happens during the remote monitoring period.

Tamper-resistance will be ensured by challenging and interrogating the sensor with a key value obtained from the bioprint which is derived from the combination of three biosensors and control sensors (for each panel in Figure 1), which is specific to the monitored patient. Furthermore, since the biosensors provide a comprehensive multimodal panel that will monitor the evolution of cardiac markers over time against the initial time (e.g. time zero stored in the doctor's office); we hypothesize that each individual will be characterized by a unique cardiac fingerprint much like a biometric fingerprint that is person-specific. The self-reference sensor will act as a blank electrode that will provide an individualized value - as a unique background current- characteristic to the biofluid sample of each individual (e.g. blood). Variability in these values among different individuals will be established experimentally.

Challenge Based Sensing to Avoid Replacement Tampering

The second tamper resistance approach we propose deals with breaches through the replacement of the healthy sensors with fake ones. We define this as *replacement tampering*. Our proposed challenge-based sensing to detect sensor-tampering is inspired by the following concepts: i) US Department of Homeland Security reports trusted cyber future as a visionary goal for the next few decades (DHS-Goals, 2015), where security is built directly into non-invasive screening devices. ii) Non-invasive tampering on anti-lock braking systems (ABS) in a car could cause the car to crash by making the ABS system think that the car is travelling slower than it actually is (Shoukry, Martin, Tabuada, & Srivastava, 2013). This can be achieved by a surprisingly simple tampering, where a thin electromagnetic actuator is placed near the ABS wheel sensors and the resulting electro-magnetic interference alters speed measurements.

As reported by the authors (Shoukry, Martin, Tabuada, & Srivastava, 2013), operating knowledge of the sensors is required against such an attack, which is used to challenge the sensory data. In our proposed remote health monitoring system, each sensor will have an electronically stored calibration curve at the potential characteristic of the electrochemical process of the electrode surface; purposely, a second calibration curve (or a few more), at a different potential range will also be recorded and stored to allow *replacement-tamper-resistance*. The purpose of these additional calibration curves is to create multiple other operating points, even if not efficient, with the intention to use them for challenging the sensor.

Although additional challenges for the sensor correspond to additional measurements, from Equation 1 we observe that, this introduces a negligible additional system power consumption. Especially since the results are being transmitted in a burst, additional challenges (i.e., redundant measurements at multiple sub-optimum operating points) do not create a noticeable communication overhead either. For example, assuming 10 redundant measurements for each actual measurement, the increase in P_{sensor} and P_{uC} is negligible, since we already assumed 100% activity for these two components. Assuming that the increase in the Zigbee activity (P_{Zigbee}) is 50% (not more, since the amount of data is very low), this only reduces the battery life to 570 hours (23 days) from the original 30 days. Different challenge scenarios and optimum challenge vs. energy consumption trade-offs are possible and they are left for future research topics.

Robust Sensing

Validity of a patient's sensed biomedical information is highly dependent on two major factors: First, the precision of the sensor measurement which is limited by the ADC quantization noise and the amplification/sensing circuitry noise. Second, the robustness of the mapping of the measured sensor response to the patient's biomedical information in the presence of general noise and variations in conditions such as temperature and the excitation voltage. Limited storage capacity on the sensing/mapping device requires applying robust methods to extract a patient's biomedical information with a minimum amount of stored data.

On the circuit side, apart from using low noise elements, efficient techniques can be applied to reduce noise levels based on the low frequency nature of measurements. Commercial off-the-shelf ADCs are able to achieve a sampling rate of the order kilo samples per second. Since measuring patient's biomedical information is carried out at a much lower frequency, over-sampling based techniques can be employed to improve the signal-to-noise ratio while keeping the number of bits in the ADC samples constant. According to Figure 3, there is a one-to-one mapping between the sensor current and the

biomarker concentration at a given applied excitation voltage. However, due to the presence of noise and limited accuracy of stored data, a single measurement may not be sufficient to describe the sensor response accurately. Measuring the sensor response at different excitation voltage levels and using a systematic approach such as Kalman filtering (Sorenson, 1970) to combine measurement results can lead to more robust and accurate mappings. Kalman filtering has been extensively used for robust estimations of unobservable variables in a variety of fields (Nadeau, Sharma, & Soyata, 2014) including medical science. For example in (Li, Mark, & Clifford, 2008), a Kalman filtering approach has been introduced for robust heart beat estimations from multiple asynchronous noisy sources.

INTERNET-OF-THINGS BASED SENSORY ARCHITECTURE

Development of cloudlet and concentrator design are two key components in Internet of Things (IoT)-based sensory architecture. This section overviews these two key enablers towards IoT-integration of the proposed system, which is indicated as "III" in **Figure 1**.

Cloudlet Design

Cloudlet is a limited-resource local computing and storage platform that eliminates outsourcing certain resource-intensive tasks to the enterprise cloud (Hoang, Niyato, & Wang, 2012; Jararweh, Tabalweh, Ababneh, & Dosari, 2013; Li & Wang, 2013; Soyata T. , et al., 2012). Cloudlet computing is a strong candidate for health monitoring applications via body area networks as it reduces the delay of accessing the enterprise cloud (Quwaider & Jararweh, 2013). Furthermore, user privacy can be substantially improved by Map-Reduce based watermarking running on a cloudlet system.

Our proposed cloudlet design adopts the Kimberly architecture which delivers VM overlays to the mobile clients in order to utilize a dedicated VM in the cloudlet (Satyanarayanan, Bahl, Caceres, & Davies, 2009). In order to perform virtualization, Oracle VM VirtualBox must be installed in the cloudlet server. VM overlay sizes must be determined empirically, however, given that the full VM image can go up to a few gigabytes, VM overlay sizes must be configured to be some hundred megabytes. On the cloudlet server, we propose to implement a pseudo-distributed single node Hadoop cluster in order to run time critical analysis of sensed data. The reason behind adopting Kimberly architecture is that the cloudlet is self-manageable and flexible for the developer. On the other hand, the downside is the overlong VM synthesis (60-90 seconds). VM overlay prefetching mechanism must be applied along with parallel compression/decompression in order to reduce the VM synthesis delay. Nevertheless, we propose a holistic and interoperable cardiac monitoring system. Therefore once it is validated, this conceptual model can be implemented on other cloudlet architectures as well such as the Clonecloud (Chun, Ihm, Maniatis, Naik, & Patti, 2011) or Mobile Assistance Using Infrastructure (MAUI) (Cuervo, et al., 2010).

Concentrator Design

With the advent of sensing based applications, billions of uniquely-identifiable embedded devices are expected to be interconnected in the Internet of Things (IoT) architecture (Aggarwal, Ashish, & Sheth,

2013), in which a concentrator acts as a communication gateway for the sensors and connects each sensor to the Internet (Vazquez & Ipina, 2008). Connecting sensors to the internet involves collecting sensed data, as well as interpretation of the data locally or at a remote host. These steps can be achieved in a cost efficient and scalable manner if cloud computing is integrated into the IoT architecture (Gubbi, Buyya, Marusic, & Palaniswami, 2013). Remote healthcare monitoring is reported to be an application domain that can benefit from cloud-IoT integration (Doukas & Maglogiannis, 2012). The sensory network infrastructure that we propose departs from this vision as shown in Figure 1 by treating the bio-sensor array as a form of an IoT infrastructure, where the HCO datacenter is a private cloud, and the cloudlet in the patient's house is a concentrator (either the patient's smartphone, or a dedicated cloudlet as in (Soyata T. , Muraleedharan, Funai, Kwon, & Heinzelman, 2012)).

Smartphones of the patient and/or the attendants can offer ideal platforms to replace the concentrators in the Internet of Things (IoT) infrastructure as current smart phones can use both LTE and WiFi as the backhaul network. Aggregation tasks can be handled either in a local cloudlet or in the HCO's datacenter. We propose context-aware concentration of the data in the cloudlet (i.e., via WiFi connectivity) or in the HCO datacenter (i.e., via LTE connectivity). The former leads to one tenth of the latter's access delay, half the power of the latter's power consumption and ten times the latter's throughput (Jararweh, Tabalweh, Ababneh, & Dosari, 2013; Wang, Liu, & Soyata, 2014). The tasks on the aggregated data will be partitioned between the cloudlet and the data center, however this research proposes context-aware partitioning of the data between these two entities. Context must be defined as a function of the current and expected status of the patient, whereas this decision making system will be implemented as an integrated component of the concentrator. Learning automata-based concentration is expected to address (i.e., adapt) the trade-off between computation and performance subject to the context, i.e., environmental dynamics (Soyata, Friedman, & Mulligan, 1997). In order to ensure fast convergence and efficiency, the concentrator will adopt the estimator algorithms applied to learning automata (Oommen, 2010).

Concentrator can be implemented as a mobile application in the mobile sensing environment. Android Software Development Kit (SDK) can be used to build the mobile application. The mobile application will be communicating with the sensory circuit through WiFi module of the mobile device and temporarily store and aggregate the sensed data based on context-aware burstification. The application will transmit the burstification through either cellular or WiFi module of the mobile device based on the time criticality metric which is denoted by the context. Communication via WiFi module will enable starting VM synthesis function in the cloudlet.

Reliable and Secure Sensing Algorithms

Sensing is proposed as a cloud-based service (Lauro, Lucarelli, & Montella, 2012; Rao, Saluia, Sharma, Mittal, & Sharma, 2012; Sheng, Tang, Xiao, & Xue, 2013), while trustworthy sensing has been studied in the context of sensor reputation-awareness and accurate sensing (Kazemi, Shahabi, & Chen, 2013; Shahabi, 2013), user privacy and data integrity (Gilbert, Cox, Jung, & Wetherall, 2010). Kantarci and Mouftah have proposed a trustworthy sensing-as-a-service architecture (Kantarci & Mouftah, 2014; Kantarci & Mouftah, 2014) for a public safety application, presenting a framework to ensure trustworthiness of the sensed data. In their proposal, sensors are recruited based on their reputation, which is defined as the percentage of correct readings after eliminating the outliers through the algorithm in

(Zhang, Meratnia, & Havinga, 2010) and adopting a Wilson score to increase the confidence of reputation calculation (Carullo, et al., 2013). Most of these ideas will be applied to the proposed system.

Trust-based data aggregation methods for wireless sensor networks (WSNs) have been studied in the literature however, most of these studies address sensing data accuracy (Sun, Luo, & Das, 2012) or detect threats on individually compromised nodes (Zhang, Das, & Liu, 2006). In our proposed system, multiple sensors are deployed in the same region and mostly in the same transmission range. This introduces resiliency issues to the sensory system where the entire sensor network can fail requiring prompt intervention. As the collected data from the sensory system is expected to be correlated with any other indicator of cardiac status, this research aims at integrating off-the-shelf heart monitoring systems (Agu, et al., 2013) into the proposed sensory system, and detect anomalies in the biosensor signals through correlation analysis.

COMMUNICATIONS ARCHITECTURE

As shown in **Figure 1**, our proposed system which consists of the data acquisition, data aggregation, and application layers. The data acquisition layer consists of the sensory circuit, the concentrator and the cloudlet. The concentrator can be implemented within a smart phone in the vicinity of the patient and the cloudlet can be implemented by a computer accessible via WiFi or a smartphone. Sensory circuit communicates with the concentrator via a IEEE 802.15.4 (Zigbee) interface as Zigbee provides low power, low cost communication in a short range. Concentrator should also use Zigbee to avoid depleting the battery power due to WiFi or LTE access (Olteanu, Oprina, Tapus, & Zeisberg, 2013; Kwon M. , 2015). The concentrator is also equipped with a WiFi interface to communicate with the cloudlet and an LTE interface to communicate with the Cloud via a mobile backhaul (Kwon, et al., 2014). Visualized data represented to the Application layer via WAN over the Internet backbone and the mobile backhaul as the doctor will be able to access the visualized data via his/her smart phone anytime and anywhere. The challenges and novel solutions for the communication infrastructure of the proposed architecture are as follows:

Urgent data aggregation tasks are handled in the cloudlet (Powers, Alling, Gyampoh-Vidogah, & Soyata, 2014). Besides designing specific cloudlet functions, this research aims at generalizing and standardizing cloudlet operation for medical data acquisition. Building blocks for cloudlet design are virtualization, standardized signaling mechanisms for admission control, resource allocation, quality of service provisioning for associated mobile devices, and resiliency of the cloudlet including security and privacy concerns. Virtualization is the most straightforward block as it will be achieved by a hypervisor implementation. The novelty of the proposed system lies on the blocks above virtualization, all of which will be designed with abstract interfaces so that any application (e.g., telemedicine, military, traffic) can request admission to the cloudlet by implementing the appropriate interface. Based on the requirements of the application, resources will be allocated by considering QoS metrics and encapsulated with security and privacy services.

Contemporary sensing systems offer integrated solutions that incorporate individual sensor design with the aggregation system. However, near-commodity acquisition system is only software, whereas the intellectual property of the telecommunication companies is embedded into the sensor design. In this chapter, we propose to decouple the acquisition software from the sensor design via a novel interoperable sensor data transmission mechanism. The interoperability mechanism will enable each party to be

interfaced through the proposed wireless sensing platform by adopting existing IEEE 1451 and ISO IEEE 11073 standards. IEEE 1451 standardizes the communication interface between sensors and micro-controllers and/or control networks whereas ISO IEEE 11073 defines communication standards between the healthcare devices and external computing resources. Our proposed system will adopt these standards and extend them towards a tamper-resistant interoperable wireless sensing platform.

Although personally-identifiable information will be removed before communicating sensed data, aggregate disclosure attacks aim at deducing information through pattern recognition methods (Abbas & Khan, 2014; Gkoulalas-Divannis, Loukides, & Sun, 2014; Alling, Powers, & Soyata, 2015). Novel algorithms must be developed to hide sensitive sequential patterns in the aggregated cardiac data. We envision the overall sensory system to be tamper-resistant, however, context-awareness may introduce privacy vulnerabilities under aggregate disclosure attacks by allowing the intruder to infer information regarding the health condition of the monitored patient based on concentrator-to-mobile-backhaul network traffic patterns even if the patient identity is not revealed. Random linear network coding along with lightweight homomorphic encryption has been shown to be efficient to overcome malicious adversaries via network analysis in multi-hop wireless networks (Fan, Zhu, Chen, & Shen, 2011), although fully homomorphic encryption is too slow for practical use (Kocabas & Soyata, 2014; Kocabas, et al., 2013; Page, Kocabas, Soyata, Aktas, & Couderc, 2014; Page, Kocabas, Ames, Venkitasubramaniam, & Soyata, 2014). We propose to adopt existing approaches (Fan, Zhu, Chen, & Shen, 2011), but to unwrap network coding from lightweight homomorphic encryption. The concentrator will be designed to employ a network coding-inspired approach to assign data aggregation tasks to the cloudlet and the HCO datacenter, thereby achieving resistance to aggregated disclosure attacks.

VISUALIZATION OF THE ACQUIRED SENSORY DATA

The previous section discussed secure methods for uploading medical sensor data to the healthcare provider. We will now explain a procedure for cleaning up the raw data and presenting it to the doctor. This is the part of our proposed system in **Figure 1**, which is denoted as "IV." Currently, doctors will review snapshots of results that may overly-simplify the true situation, or otherwise miss vital pieces of the full picture. For example, with ECG, a cardiologist may never see what happens to your heart rate during sleep, because he only checks it while you're present during clinic hours. With 24-hour monitoring data, we can look at these periods. However, we still need to greatly compress the information so that the doctor can read a summary in a few seconds; we cannot give him a list of the patient's heart rate for all of yesterday's 100,000 heart beats, for example, nor should we simply average them to produce a single number. Visualization techniques must be developed that can quickly present long-term data while preserving all important information and revealing problems that conventional techniques would have missed. This will require massive computation and filtering in the cloud, and experimentation to determine the most useful way to display the results. We now present a case study to illuminate this process.

Background / Case Study

One application that can greatly benefit from long-term monitoring is diagnosis of the Long QT Syndrome (LQTS). This is a disorder that may be drug induced or genetic, and is easy to detect from an ECG signal. **Figure 7** illustrates the relevant intervals on an ECG. As the QT interval becomes more

prolonged relative to the RR interval, risk of potentially-fatal arrhythmias such as torsades de pointes (TdP) is greatly increased (Shah, 2004). To evaluate this risk, the QT and RR intervals are typically merged into a single variable, QTc, which is the *corrected* QT based on RR. Two typical correction equations are:

$$QTcB = \frac{QT}{\sqrt{RR / \text{sec}}}$$

and

$$QTcF = \frac{QT}{\sqrt[3]{RR / \text{sec}}}$$

where the ‘B’ and ‘F’ indicate that these are the Bazett (Bazett, 1920) and Fridericia (Fridericia, 1920) corrections, and the division by 1 second is to preserve the units of QT. There are gender-dependent thresholds above which a patient’s QTc is considered dangerous. While there is no universal standard for these thresholds, they are generally around 450ms-470ms. When evaluating a patient’s QTc, a cardiologist will usually review a 10-second ECG snapshot, or possibly a single daily average.

The genetic mutations that can cause LQTS are denoted LQT1, LQT2, ... LQT13 (Hedley, et al., 2009). LQT2 and LQT3 tend to cause more problems at night (Stramba-Badiale, et al., 2000), when the heart rate is low (i.e. when RR is high), meaning that the single average QTc value reviewed by the doctor is unlikely to show the full scope of a patient’s LQTS. When a subject has periods of prolonged QT that are not always present, we say that they have *concealed* LQTS. Additionally, certain prescription drugs can prolong QT in ways that may not be fully characterized during clinical tests, resulting in more prolongation when the patient goes home than the doctor was able to predict from in-hospital monitoring. To better detect and treat patients in these situations, we envision a long-term remote-monitoring system that can upload ECG signals to the healthcare provider for automated analysis of QTc. Ideally, this system will provide a 24-hour picture to the doctor in a simple form containing all key information; i.e. we want to summarize, while avoiding under-sampling or over-averaging of the data.

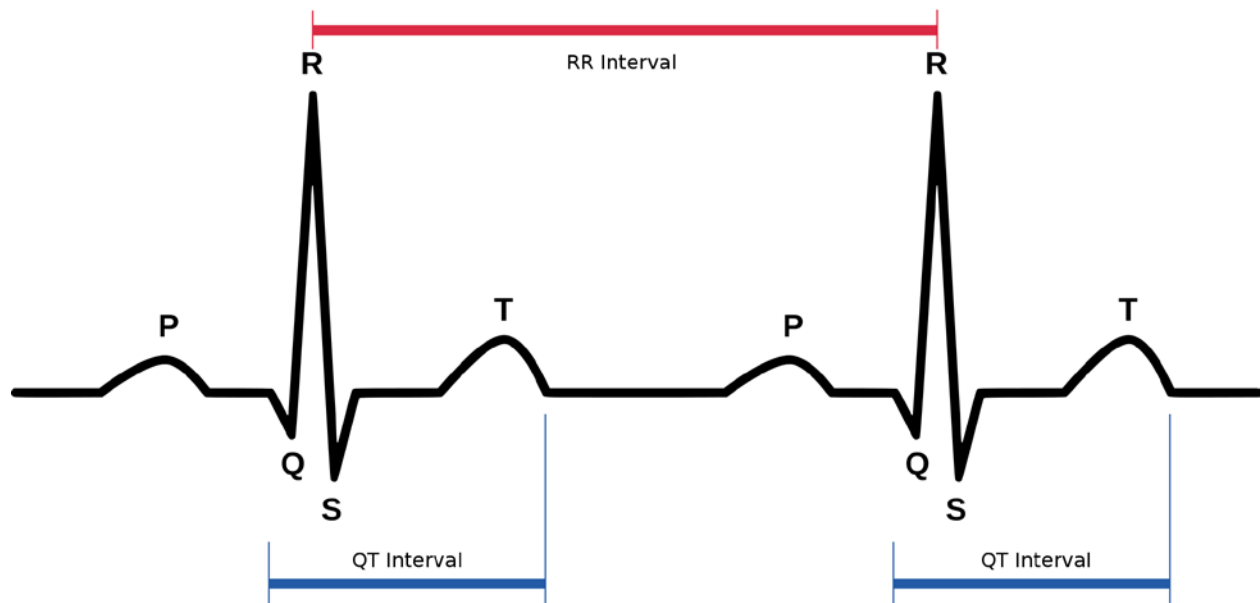


Figure 7: Typical ECG trace, with QT and RR intervals labeled. (Image based on SinusRhythmLabels.png by Anthony Atkielski.)

Components

The process we have just introduced requires several stages. First, sensor data must be collected and stored in a standardized way. Existing standards may be very different across technologies, so another standardization layer may be necessary to simplify access to heterogeneous sensor data. Once the data is organized for easy access, we need to know what features a doctor will be interested in. Heart rate, for example, is very likely to be of interest. Some ECG sensors may output this directly, but they may simply annotate where each beat occurred, or give RR rather than heart rate. Or, in the worst case, they may only give us amplitude (voltage) vs. time. In all of the latter cases, calculations are required to get the heart rate, and the cloud and/or cloudlet should therefore immediately start computing and storing it for rapid retrieval. Other features (such as the PR interval) may not be as useful, so we may choose only to compute them on demand rather than wasting time and storage up front.

To collect ECG data over 24 hours or more, the standard method is a Holter monitor (Holter, 1961). A Holter monitor is a portable ECG device that records data for later retrieval and review, usually on 2-3 separate sensors (which are typically referred to as *leads*). Many other portable ECG devices are now available, such as the AliveCor Heart Monitor (AliveCor, 2014) and the Clearbridge VitalSigns CardioLeaf (CardioLeaf, 2013). These devices take care of the data collection and upload portions of our system. However, for this proof of concept, we will simply download Holter recordings from the THEW database (Couderc, 2010). One of the main advantages to this approach is the availability of ECG recordings from known LQTS patients, which allows us to test our analysis and visualization processes on relevant data.

From the raw ECG data (in ISHNE format (Badilini, 1998)), we must build a hierarchical database that has the original data at its lowest layer, commonly-requested features such as heart rate at

the highest layer, and primitives such as “R peak locations” in between. This structure allows us to generate results more quickly than building them from the raw data on every request, and it also allows us to standardize the interface to clinically-relevant features at the highest layers when dealing with different types of sensors. We construct the database for our LQTS application in two major steps:

1. ISHNE-formatted ECG recordings are converted to annotations of every feature in the recording; these annotations include the lead, location, and amplitude for features such as Q, R, and S in every heartbeat. These are the ‘primitives’ mentioned above; from them, we should be able to calculate almost any result without returning to the original data. This annotation is performed by an open-source C++ library (Chesnokov, Nerukh, & Glen, 2006). The results for each recording are then stored in a SQLite (SQLite, 2015) database corresponding to that recording. In the long term, a different database system such as MySQL (MySQL, 2015) or MariaDB (MariaDB, 2015) will likely be a better solution, but for now, SQLite simplifies portability across our test systems.
2. From the primitives computed in step 1, we can now compute the values of interest such as QT and heart rate. Although these computations are relatively simple – e.g. subtracting Q from T – there are ~100,000 heart beats per patient per day, detected on 3 separate leads. This begins to add up to a lot of computation if we wait until the doctor asks for it. Further, if we want to aggregate results, perhaps to see the average heart rate for a group of 1000 people, we are much better off having pre-computed it across each recording. So this step will save a lot of time for future queries. These results are stored in a separate table in the SQLite database associated with each recording.

While building this database, we can take advantage of redundant ECG sensors to clean things up a bit. If ‘R’ was detected on 3 different leads in the original recording, for example, we may use the *median* R value to calculate RR. Or, we may choose to average each value across all leads, weighed by their signal quality. In this way, we can keep the higher layers of the database leaner and more accurate.

The final component in the overall system is the “frontend” part, which will use the database to generate tables and plots. We perform the computation and plotting for this final stage mainly using NumPy (NumPy, 2015) and matplotlib (matplotlib, 2015). The details are discussed in the following section.

Output / Filtering

One useful result that can be drawn from the database we’ve constructed is a view of the typical range for a given feature over 24 hours – either for a single patient, or the average for a population. For example, we may want to see how much heart rate decreases at night compared to during the day, and also how its variability changes. One way to visualize this is with a plot of heart rate vs. time, as seen in Figure 8.

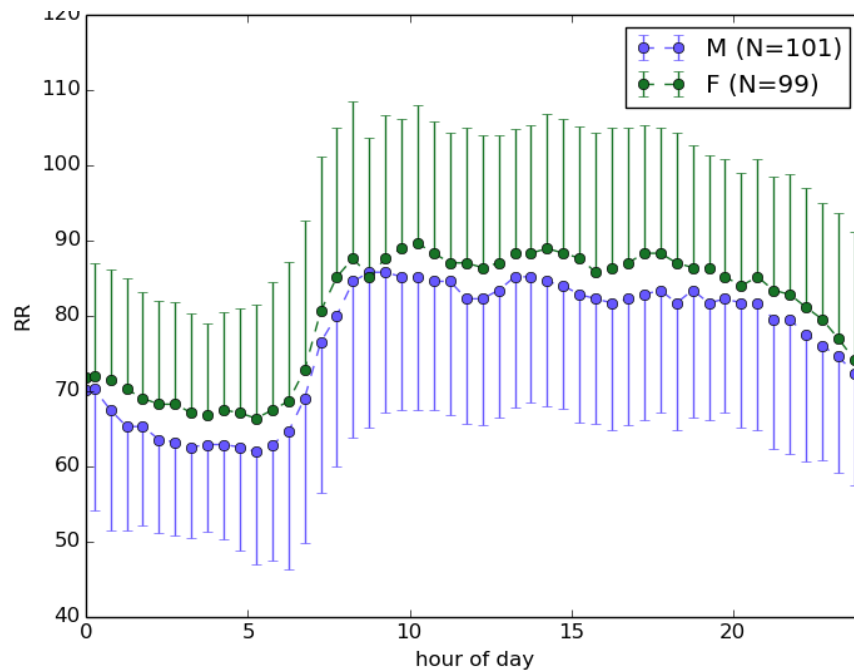


Figure 8: Median heart rate (beats per minute) in healthy subjects, male vs. female. Error bars indicate standard deviation, and are drawn in only one direction to avoid overlap. RR is in beats per minute, and hours are indexed from midnight. Results generated from THEW E-HOL-03-0202-003 database.

While this format is instructive, we have found that conventional Cartesian plots are somewhat cumbersome to interpret due to the discontinuities at the endpoints and the inconsistent or inconvenient placement of the origin in terms of time-of-day. Plots of 24-hour data are much more intuitive on polar axes, once the viewer becomes accustomed to this style. In polar coordinates, we use the angle to indicate time of day and the radius to indicate the value of a feature (such as QTc). We have also found that it is best to maintain fixed axes ranges for any particular feature, e.g. 300ms-600ms for QTc, so that the viewer doesn't need to adjust to a new scale for each plot. Some examples of this technique are given in Figure 9, Figure 10, and Figure 11.

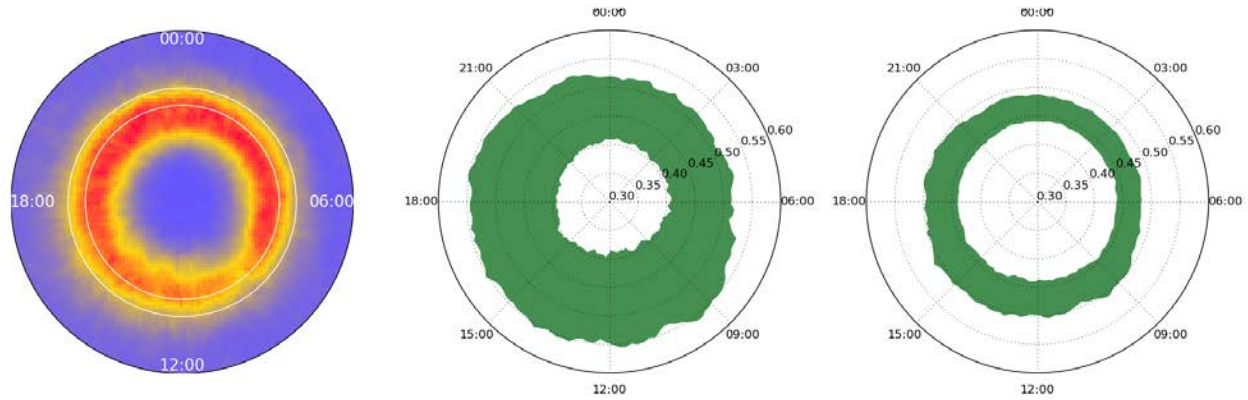


Figure 9: Visualizing the typical range of values for a feature. These 3 plots are for QTcB in LQT1 female subjects who are not on beta blockers. Left: histogram of QTcB for all heart beats, with white circles at radii of 470ms and 500ms (“warning” and “danger” for females). Center: median QTcB +/- 1 standard deviation. Right: median QTcB +/- median absolute deviation. Results generated from THEW E-HOL-03-0480-013 database.

In the histogram in Figure 9, we have plotted QTcB for every heartbeat from 94 24-hour recordings –approximately 10 million data points in total. We then produce a similar plot showing points within 1 standard deviation of the median as a solid color. Median is used rather than mean because we expect to have a non-negligible number of erroneous values in our data set due to the noisy environment and imperfect annotation algorithm, and we want to avoid giving weight to these bad values. However, these outliers still affect the standard deviation; the width of the band in the center plot is a result of this. Further, the standard deviation across multiple patients gives a false sense of how much variability is really normal for a single patient. To get a more representative view of QTcB, we produce the same plot using median absolute deviation (MAD) instead of standard deviation. This results in the final plot in Figure 9.

Next, we would like to look at a single patient’s QTc, and compare it to their peers (or to a healthy population). The first plot in Figure 10 illustrates the effects of noise when we attempt to simply view QTcB vs. time on one of our “clock” plots. Noise is not washed out like it was in the histogram; a line is being drawn to every outlier, and even relatively small error rates can produce a few thousand outliers over the course of a day (which consists of ~100,000 heart beats). This is amplified by the fact that a single faulty detection can result in two incorrect values; with heart rate, for example, wrongly detecting an extra heart beat would make the heart rate appear to jump up for 2 beats and then return to normal. Further, QTc is somewhat dynamic; much of its variation isn’t “noise,” it’s real. To smooth the plot, we apply a median filter to the list of QTc values, replacing each point with the median of the points around it. The impact of this filtering process is shown in the remaining plots in Figure 10. This approach will cause problems, though, if the doctor is interested in short-duration events; events that occur for less than ~5 minutes, for example, are likely to be removed by the filter. The best solution for this is to collect a cleaner signal (e.g. using better sensors) and to apply more advanced annotation techniques. It is also important to eliminate errors at each stage in the database construction. Because there are so many data points to work with, it is generally safe to discard all questionable values.

Relatively wide filters do not cause a problem for the QTc case study, but physicians will need to select filtering windows that make sense for their application.

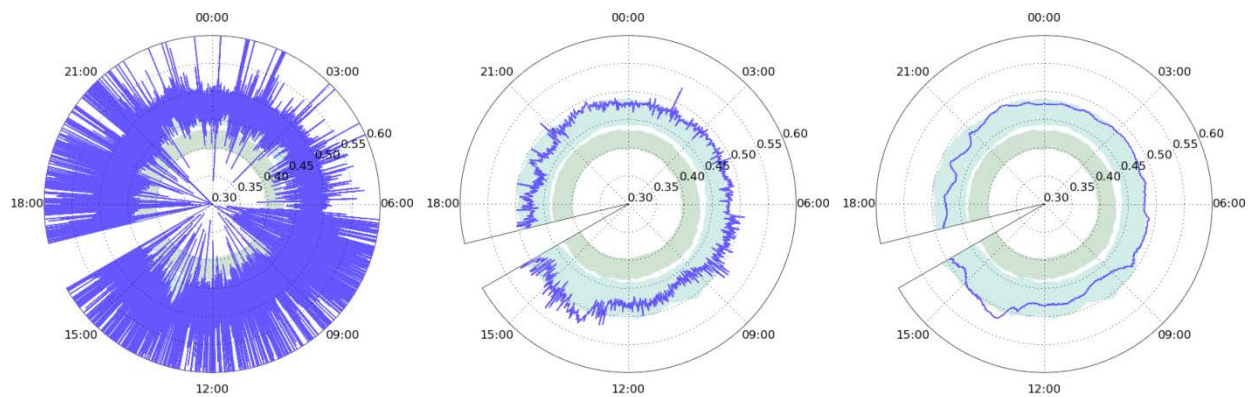


Figure 10: QTcB extracted from Holter recording of a 32yo female LQT1 patient. Left: unfiltered. Center: sliding window median filter, width = 2 minutes. Right: sliding window median filter, width = 20 minutes. Green background: typical range for healthy female subjects. Turquoise background: typical range for female LQT1 subjects. The ‘notch’ around 4-5PM was not recorded.

At this point, we have accomplished the main goal of our case study: to present 24 hours of QTc information to the doctor in a concise and useful form. One of the intended applications for this tool was detection of concealed LQTS. As we mentioned earlier, doctors normally only check a patient’s QTc for a few seconds during the day, or as an average value over a longer period of time. Figure 11 shows two cases where current methods would fail to reveal the full extent of a patient’s QT prolongation, but our “QTc clock” reveals it immediately. The plots in this figure only take a few seconds for the doctor to review, which is important for a physician who may have 20 or more patients to check on each day, and who will likely want to review other features (e.g. heart rate) as well.

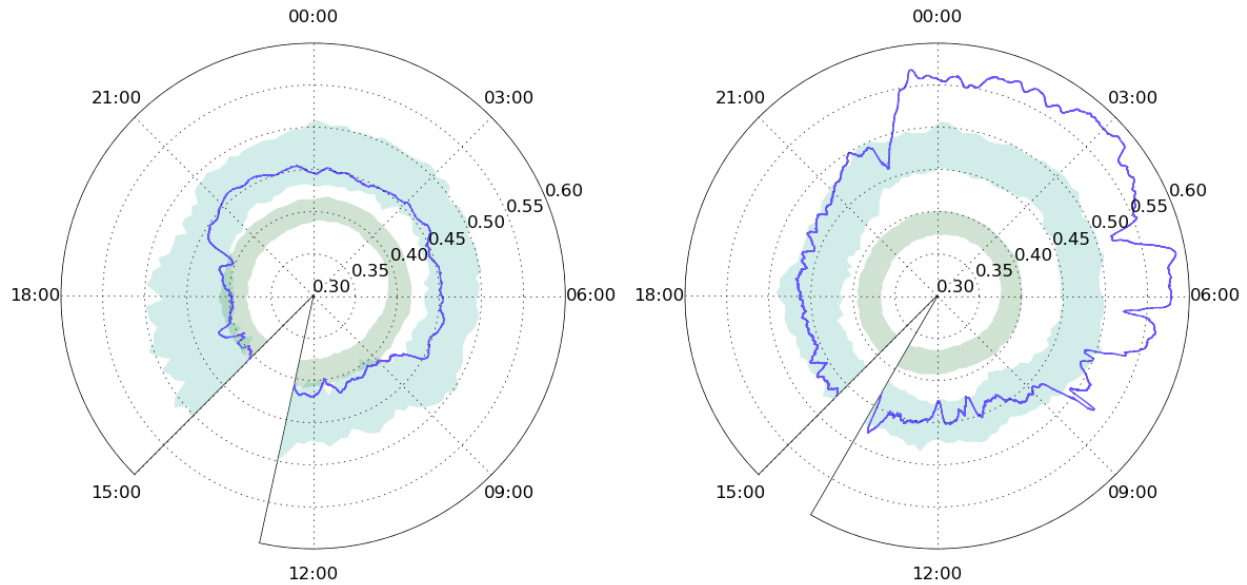


Figure 11: QTc in LQT2 patients exhibiting LQTS concealment during the day. Left: 1yo female, not on beta blockers. Right: 38yo male on beta blockers. Green background: typical range for healthy individuals of same gender. Turquoise background: typical range for patients with same gender and LQT genotype. Note that the nocturnal QTc of these patients would not be seen during clinic hours. Further note that some nighttime QTc prolongation in these populations is normal, as shown by the asymmetry of the turquoise bands.

Implications and Future Research Directions

We have shown that doctors can use the QTc clocks to detect concealed LQTS, but these plots have many other uses as well. They can reveal whether a patient is taking certain prescriptions correctly or not, if a prescription should be adjusted, or even what dose is likely to be safe for someone being started on a new drug. Further, the database we've developed can be used for purposes other than visualization, such as decision support. The increased availability of sensor data from a wide variety of patients will yield very refined characterizations of specific groups, differentiated by genetic mutation types, drug use, age, etc., allowing software to make diagnosis recommendations and even to predict the effects a prescription would have on a certain patient. Finally, we remind the reader that long-term QTc monitoring is only one example of a medical data visualization problem. The same techniques we've presented can immediately be extended to other features (such as heart rate) and other sensors (such as glucose monitors). Without these tools, the increasing volume of sensor data will become overwhelming to the clinicians who need to process it.

CONCLUSIONS AND FUTURE WORK

In this chapter, we proposed a real-time remote patient monitoring system for cardiac conditions. Such a system does not exist in today's technology both in terms of the difficulty in standardizing data acquisition formats and systems, and the strict regulations governing the medical arena. The design of such a system has the potential to revolutionize the patient care since it can provide real-time data to health professionals in a summarized format. While the design of the individual components of such a system is feasible in today's technology, integration of these individual pieces requires a lot more effort to result in a practical system. In this chapter we described the components that we deem necessary in detail.

First component we described is a set of novel biosensors that can detect non-trivial biomarkers related to the diagnosis of deadly cardiac conditions. We analyzed the detection of these biomarkers in two distinct categories: the i) Protein and ii) Oxidative Stress panels. In the protein panel (i), we detailed the design of a biosensor array for detecting such biomarkers as Cardiac Troponin (cTn), C-reactive protein (CRP), and Myoglobin (MYO). In the Oxidative Stress panel (ii), we described the design of a second biosensor array capable of measuring Cholesterol(Ch), superoxide radicals (O_2^-) and nitric oxide (NO) levels.

The second component we described is a custom sensor-interface circuitry which interfaces with these two biosensor arrays and reports the measurement results to the communication infrastructure using the low-power Zigbee communication protocol. As a crucial part of the circuit design, we described how to take advantage of the knowledge of the electrochemical properties of the six biosensors to achieve tamper-resistance. We introduced two separate methods for achieving tamper-resistance: i) by adding a blank control electrode to each panel in both sensor arrays, thereby increasing the total number of sensors to eight in the entire system. The addition of the control sensors can facilitate the establishment of individualized bioprints for each patient, thereby enabling the identification of our first conceptualized tamper scenario which we defined as *relocation tampering*. ii) by performing redundant measurements during the sensing process for the purpose of identifying the validity of the results to these additional measurements. This will enable the detection of the second kind of tampering which we defined as *replacement tampering*, in which a sensor is placed with a fake one by an adversary. Since the adversary will not be able to answer the additional measurements (which we called *challenges*) correctly, we can detect the breach and ignore even the correct results.

The third component we described is the communication architecture which is composed of an Internet-of-Things (IoT)-like sensor array, followed by a concentrator to collect and accumulate the results from multiple sensors. Within this communication infrastructure we described the functionality of a cloudlet, which is a device that is capable of performing non-trivial computations at the site of data acquisition. We proposed to utilize the cloudlet to perform sensor interrogations controlled by the algorithms that are stored in the cloud. The final destination of the acquired data, after being aggregated by the concentrator and verified by the cloudlet is the HCO's datacenter, which can be considered to be a private cloud. This proposed communication architecture places the *application intelligence* inside the cloud, based on our conceptualization that, the most privacy-vulnerable of this system is the least computationally-capable portion of it, which is the sensory acquisition IoT network. Therefore, our proposed system can achieve arbitrarily high levels of privacy, constrained only by the capabilities of the sensory network. In other words, the development of an ever-increasing set of sophisticated cloud-cloudlet-concentrator algorithms is possible with an increasing number of *software-knobs* provided by the sensory network.

The final components of our system is the visualization of the acquired data once it is stored in the private cloud. We proposed novel methodologies for visualizing long-term monitoring results which permits a doctor to visualize data for multiple patients within seconds. An example of QTc (corrected QT) monitoring over a 24 hour period is described where, by using intuitive colored bands, a doctor can immediately see abnormal cardiac functionality. Future research includes the visualization using the same

scheme, albeit with an increased number of co-plotted biomarkers. While the visualization of a single biomarker (QTc) provided a very intuitive way to monitor patient health, adding an increasing number of biomarkers to the same plot (e.g., Cholesterol, Troponin) will require further investigation. We believe that, the proposed system in this chapter has the potential to revolutionize the healthcare of the 21st century.

ACKNOWLEDGMENT

This work was supported in part by the National Science Foundation grant CNS-1239423 and a gift from Nvidia corporation.

REFERENCES

- Abbas, A., & Khan, S. (2014). A review on the state-of-the-art privacy-preserving approaches in the e-health clouds. *IEEE Journal of Biomedical and Health Informatics*, 1431-1441.
- ADI-ReportADC. (2015). *ANALOG-DIGITAL CONVERSION*. Analog Devices, Inc. Retrieved from <http://www.analog.com/library/analogDialogue/archives/39-06/Chapter%20%20Sampled%20Data%20Systems%20F.pdf>
- Aggarwal, C., Ashish, N., & Sheth, A. (2013). The internet of things: A survey from the data-centric perspective. *Managing and Mining Sensor Data*, (pp. 383-428).
- Agu, E., Pedersen, P., Strong, D., Tulu, B., He, Q., Wang, L., & Li, Y. (2013). The smartphone as a medical device. *10th Annual IEEE Communications Society Conference on Sensor, Mesh and Ad Hoc Communications and Networks (SECON)*, (pp. 76-80).
- AliveCor. (2014). *AliveCor Heart Monitor*. Retrieved from <http://www.alivecor.com/home>
- Alkasir, R. S., Ganesana, M., Won, Y. H., Stanciu, L., & Andreescu, S. (2010). Enzyme functionalized nanoparticles for electrochemical biosensors: a comparative study with applications for the detection of bisphenol a. *Biosensors and Bioelectronics*, 43-49.
- Alkasir, R. S., Ornatska, M., & Andreescu, S. (2012). Colorimetric paper bioassay for the detection of phenolic compounds. *Analytical chemistry*, 972909737.
- Alling, A., Powers, N., & Soyata, T. (2015). Face Recognition: A Tutorial on Computational Aspects. In *Emerging Research Surrounding Power Consumption and Performance Issues in Utility Computing*. Hershey, Pennsylvania: IGI Global.
- Andreescu, S., Barthelmebs, L., & Marty, J. L. (2002). Immobilization of acetylcholinesterase on screen-printed electrodes: comparative study between three immobilization methods and applications to the detection of organophosphorus insecticides. *Analytica Chimica Acta*, 171-180.

- Andreescu, S., Magearu, V., Lougarre, A., Fournier, D., & Marty, J. L. (2001). Immobilization of enzymes on screen-printed sensors via an histidine tail. application to the detection of pesticides using modified cholinesterase. *Analytical letters*, 529-540.
- Babko, A., & Volkova, A. (1954). The colored peroxide complex of cerium. *Ukrains' kii Khemichnii Zhurna*, 211-215.
- Badilini, F. (1998). The ISHNE holter standard output file format. *Annals of noninvasive electrocardiology*, 263-266.
- Bazett, H. C. (1920). An Analysis of Time Relations of the Electrocardiogram. *Heart*, 353-370.
- CardioLeaf. (2013). *Clearbridge VitalSigns CardioLeaf PRO*. Retrieved from <http://www.clearbridgevitalsigns.com/pro.html>
- Carullo, G., Castiglione, A., Cattaneo, G., Santis, A., Fiore, U., & Palmieri, F. (2013). Feeltrust: Providing trustworthy communications in ubiquitous mobile environment. *IEEE 27th International Conference on Advanced Information Networking and Applications (AINA)*, (pp. 1113-1120).
- Chesnokov, Y., Nerukh, D., & Glen, R. (2006). Individually adaptable automatic QT detector. *Computers in Cardiology* (pp. 337-340). IEEE.
- Chun, B. G., Ihm, S., Maniatis, P., Naik, M., & Patti, A. (2011). Clonecloud: Elastic execution between mobile device and cloud. *Proceedings of the Sixth Conference on Computer Systems*, (pp. 301-314).
- Cortina-Puig, M., Scangas, A. C., Marchese, Z. S., Andreescu, S., Marty, J. L., & Calas-Blanchard, C. (2010). Development of a xanthine oxidase modified amperometric electrode for the determination of the antioxidant capacity. *Electroanalysis*, 2429-2433.
- Couderc, J. (2010). The telemetric and holter ECG warehouse initiative (THEW). A data repository for the design, implementation and validation of ECG-related technologies. *Annual International Conference of the IEEE Engineering in Medicine and Biology Society (EMBC)*, 6252-6255.
- CR2032. (n.d.). Retrieved from http://en.wikipedia.org/wiki/CR2032_battery
- Cuervo, E., Balasubramaniam, A., Cho, D., Wolman, A., Saroiu, S., Chandra, R., & Bahl, P. (2010). MAUI: Making Smartphones last longer with code offload. *Proceedings of the 8th International Conference on Mobile Systems, Applications, and Services*, (pp. 49-62).
- DHS-Goals. (2015). *US Department of Homeland Security. Visionary Goals*. Retrieved from <http://www.dhs.gov/science-and-technology/visionary-goals>
- Doukas, C., & Maglogiannis, I. (2012). Bringing IoT and cloud computing towards pervasive healthcare. *Sixth International Conference on Innovative Mobile and Internet Services in Ubiquitous Computing (IMIS)*, (pp. 922-926).

- Fan, Y., Zhu, H., Chen, J., & Shen, X. (2011). Network coding based privacy preservation against traffic analysis in multi-hop wireless networks. *IEEE Transactions on Wireless Communications*, 834-843.
- Fridericia, L. S. (1920). Die Systolendauer im Elektrokardiogramm bei normalen Menschen und bei Herzkranken. *Acta Medica Scandinavica*, 469-486.
- Ganesana, M., Erlichman, J. S., & Andreescu, S. (2012). Real-time monitoring of superoxide accumulation and antioxidant activity in a brain slice model using an electrochemical cytochrome c biosensor. *Free Radical Biology and Medicine*, 2240-2249.
- Ge, B., & Lisdat, F. (2002). Superoxide sensor based on cytochrome c immobilized on mixed-thiol SAM with a new calibration method. *Analytica Chimica Acta*, 53-64.
- Gekakis, N., Nadeau, A., Hassanalieragh, M., Chen, Y., Liu, Z., Honan, G., . . . Soyata, T. (2015). Modeling of Supercapacitors as an Energy Buffer for Cyber-Physical Systems. In *Cyber Physical Systems - A Computational Perspective*. Boca Raton, Florida: CRC.
- Gilbert, P., Cox, L. P., Jung, J., & Wetherall, D. (2010). Toward trustworthy mobile sensing. *ACM Proceedings of the Eleventh Workshop on Mobile Computing Systems and Applications*, (pp. 31-36).
- Gkoulalas-Divannis, A., Loukides, G., & Sun, J. (2014). Toward smarter healthcare: Anonymizing medical data to support research studies. *IBM Journal of Research and Development*, 1-11.
- Gonzales, S., White, G., & Safranek, T. (2014). Near-realtime assessment of cardiovascular disease risk factors in nebraska by using essence. *Online Journal of Public Health Informatics*, 103-104.
- Gubbi, J., Buyya, R., Marusic, S., & Palaniswami, M. (2013). Internet of things (iot): A vision, architectural elements. *Future Gener. Comput. Syst.*, 1645-1660.
- Hassanalieragh, M., Soyata, T., Nadeau, A., & Sharma, G. (2014). Solar-Supercapacitor Harvesting System Design for Energy-Aware Applications. *Proceedings of the 27th IEEE International System-on-Chip Conference (IEEE SOCC)*. Las Vegas, NV.
- Hayat, A., & Andreescu, S. (2013). Nanoceria particles as catalytic amplifiers for alkaline phosphatase assays. *Analytical chemistry*, 10028-10032.
- Hayat, A., Andreescu, D., Bulbul, G., & Andreescu, S. (2014). Redox reactivity of cerium oxide nanoparticles against dopamine. *Journal of colloid and interface science*, 240-245.
- Hayat, A., Bulbul, G., & Andreescu, S. (2014). novel colorimetric approach for the detection of enzyme activity. *Biosensors and Bioelectronics*, 334-339.

- Hayes, S. A., Yu, P., OKeefe, M. J., & Stoffer, J. O. (2002). The phase stability of cerium species in aqueous systems i. e-ph diagram for the ce hclo 4 h 2 o system. *Journal of the Electrochemical Society*, C623-C630.
- Hedley, P. L., Jrgensen, P., Schlamowitz, S., Wangari, R., Moolman-Smook, J., Brink, P. A., . . . Christiansen, M. (2009). The genetic basis of long qt and short qt syndromes: A mutation update. *Human Mutation*, 1486-1511.
- Hoang, D. T., Niyato, D., & Wang, P. (2012). Optimal admission control policy for mobile cloud computing hotspot with cloudlet. *IEEE Wireless Communications and Networking Conference (WCNC)* (pp. 3145-3149). IEEE.
- Holter, N. (1961). New Method for Heart Studies: Continuous electrocardiography of active subjects over long periods is now practical. *Science*, 134(3486), 1214-1220.
- Ispas, C., Njagi, J., Cates, M., & Andreescu, S. (2008). Electrochemical studies of ceria as electrode material for sensing and biosensing applications. *Journal of the Electrochemical Society*, F169-F176.
- Istamboulie, G., Andreescu, S., Marty, J. L., & Noguier, T. (2007). Highly sensitive detection of organophosphorus insecticides using magnetic microbeads and genetically engineered acetylcholinesterase. *Biosensors and Bioelectronics*, 506-512.
- Jararweh, Y., Tabalweh, L., Ababneh, F., & Dosari, F. (2013). Resource efficient mobile computing using cloudlet infrastructure. *IEEE Ninth International Conference on Mobile Ad-hoc and Sensor Networks (MSN)* (pp. 373-377). IEEE.
- Jiao, F. F., Fung, C. S., Wong, C. K., Wan, Y. F., Dai, D., Kwok, R., & Lam, C. L. (2014). Effects of the multidisciplinary risk assessment and management program for patients with diabetes mellitus (rampdm) on biomedical outcomes, observed cardiovascular events and cardiovascular risks in primary care: a longitudinal comparative study. *Cardiovascular Diabetology*, 1-10.
- Juntilla, M. J., Tikkanen, J. T., Kentta, T., Anttonen, O., Aro, A. L., Porthan, K., . . . Huikuri, H. (2014). Early repolarization as a predictor of arrhythmic and nonarrhythmic cardiac events in middle-aged subjects. *Heart rhythm : the official journal of the Heart Rhythm Society*, 1701-1706.
- Kantarci, B., & Mouftah, H. (2014). Trustworthy crowdsourcing via mobile social networks. *IEEE Global Communications Conference (GLOBECOM)*, (pp. 1-6).
- Kantarci, B., & Mouftah, H. (2014). Trustworthy sensing for public safety in cloud-centric internet of things. *IEEE Internet of Things Journal*, 360-368.
- Kazemi, L., Shahabi, C., & Chen, L. (2013). Trustworthy query answering with spatial crowdsourcing. *Proceedings of the 21st ACM SIGSPATIAL International Conference on Advances in Geographic Information Systems*, (pp. 314-323).

- Kobza, R., Cuculi, F., Abacherli, R., Toggweiler, S., Suter, Y., Frey, F., . . . Erne, P. (2014). Twelve-lead electrocardiography in the young. *Heart rhythm : the official journal of the Heart Rhythm Society*, 2018-2022.
- Kocabas, O., & Soyata, T. (2014). Medical Data Analytics in the cloud using Homomorphic Encryption. In *Handbook of Research on Cloud Infrastructures for Big Data Analytics* (pp. 471-488). Hershey, Pennsylvania, US: IGI Global.
- Kocabas, O., Soyata, T., Couderc, J.-P., Aktas, M., Xia, J., & Huang, M. (2013). Assessment of Cloud-based Health Monitoring using Homomorphic Encryption. *Proceedings of the 31st IEEE International Conference on Computer Design (ICCD)*, (pp. 443-446). Ashville, VA, USA.
- Kundu, E. A. (2012). Oxidative stress as a potential biomarker for determining disease activity in patients with rheumatoid arthritis. *Free radical research*, 1482-1489.
- Kwon, M. (2015). A Tutorial on Network Latency and its Measurements. Hershey, Pennsylvania: IGI Global.
- Kwon, M., Dou, Z., Heinzelman, W., Soyata, T., Ba, H., & Shi, J. (2014). Use of Network Latency Profiling and Redundancy for Cloud Server Selection. *Proceedings of the 7th IEEE International Conference on Cloud Computing (IEEE CLOUD 2014)*, (pp. 826-832). Alaska.
doi:10.1109/CLOUD.2014.114
- Lauro, R., Lucarelli, F., & Montella, R. (2012). Sias - sensing instrument as a service using cloud computing to turn physical instrument into ubiquitous service. *IEEE 10th International Symposium on Parallel and Distributed Processing with Applications (ISPA)*, (pp. 861-862).
- Li, Q., Mark, R. G., & Clifford, G. D. (2008). Robust heart rate estimation from multiple asynchronous noisy sources using signal quality indices and a Kalman filter. *Physiol Meas*, pp. 15-32.
- Li, Y., & Wang, W. (2013). The unheralded power of cloudlet computing in the vicinity of mobile devices. *IEEE Globecom Workshops (GC Wkshps)*, (pp. 4994-4999).
- Lin, W. H., Zhang, H., & Zhang, Y. T. (2013). Investigation on cardiovascular risk prediction using physiological parameters. *Computational and Mathematical Methods in Medicine*, 1-21.
- Loon, M. S., Eurlings, J. G., Winkens, B., Elwyn, G., Grol, R., Steenkiste, B., & Weijden, T. (2011). Small but important errors in cardiovascular risk calculation by practice nurses: A cross-sectional study in randomised trial setting. *International Journal of Nursing Studies*, 285-291.
- MariaDB. (2015). Retrieved from <https://mariadb.org/>
- matplotlib. (2015). Retrieved from <http://matplotlib.org/>

- MAX4372. (n.d.). *Low-Cost, UCSP/SOT23, Micropower, High-Side Current-Sense Amplifier with Voltage Output*. Retrieved from <http://datasheets.maximintegrated.com/en/ds/MAX4372-MAX4372T.pdf>
- MySQL. (2015). Retrieved from <http://www.mysql.com/>
- Nadeau, A., Sharma, G., & Soyata, T. (2014). State-of-charge Estimation for Supercapacitors: A Kalman Filtering Formulation. *Proceedings of the 2014 IEEE International Conference on Acoustics, Speech and Signal Processing (ICASSP 2013)*, (pp. 2213-2217). Florence, Italy.
- Ndumele, C. D., Baer, H. J., Shaykevich, S., Lipsitz, S. R., & Hicks, L. S. (2012). Cardiovascular disease and risk in primary care settings in the united states. *The American Journal of Cardiology*, 521-526.
- NIST:FIPS-197. (2001). *Advanced encryption standard (AES)*. National Institute of Standards and Technology.
- Njagi, J., Ball, M., Best, M., Wallace, K. N., & Andreescu, S. (2010). Electrochemical quantification of serotonin in the live embryonic zebrafish intestine. *Analytical chemistry*, 1822-1830.
- Njagi, J., Ispas, C., & Andreescu, S. (2008). Mixed ceria-based metal oxides biosensor for operation in oxygen restrictive environments. *Analytical chemistry*, 7266-7274.
- Nojiri, H., Shimizu, T., Funakoshi, M., Yamaguchi, O., Zhou, H., Kawakami, S., . . . Ishikawa, H. (2006). Oxidative stress causes heart failure with impaired mitochondrial respiration. *Journal of Biological Chemistry*, 33789-33801.
- NumPy. (2015). Retrieved from <http://www.numpy.org/>
- Olteanu, A. C., Oprina, G. D., Tapus, N., & Zeisberg, S. (2013). Enabling mobile devices for home automation using Zigbee. *19th International Conference on Control Systems and Computer Science (CSCS)*, (pp. 189-195).
- Oommen, B. (2010). Recent advances in learning automata systems. *2nd International Conference on Computer Engineering and Technology (ICCET)*, (pp. 724-735).
- Ornatska, M., Sharpe, E., Andreescu, D., & Andreescu, S. (2011). Paper bioassay based on ceria nanoparticles as colorimetric probes. *Analytical chemistry*, 4273-4280.
- Otani, H. (2004). Reactive oxygen species as mediators of signal transduction in ischemic preconditioning. *Antioxidants and Redox Signaling*, 449-469.
- Ozel, R. E., Ispas, C., Ganesana, M., Leiter, J., & Andreescu, S. (2014). Glutamate oxidase biosensor based on mixed ceria and titania nanoparticles for the detection of glutamate in hypoxic environments. *Biosensors and Bioelectronics*, 397-402.
- Page, A., Kocabas, O., Ames, S., Venkitasubramaniam, M., & Soyata, T. (2014). Cloud-based Secure Health Monitoring: Optimizing Fully-Homomorphic Encryption for Streaming Algorithms. *IEEE*

Globecom 2014 Workshop on Cloud Computing Systems, Networks, and Applications (CCSNA).
Austin, TX.

Page, A., Kocabas, O., Soyata, T., Aktas, M., & Couderc, J.-P. (2014). Cloud-Based Privacy-Preserving Remote ECG Monitoring and Surveillance. *Annals of Noninvasive Electrocardiology*.

Petr, E. J., Ayers, C. R., Pandey, A., Lemos, J. A., Powell-Wiley, T., Khera, A., . . . Berry, J. D. (2014). Perceived lifetime risk for cardiovascular disease (from the dallas heart study). *The American Journal of Cardiology*, 53-58.

PIC16F1783. (n.d.). *PIC16F1783 28-Pin 8-Bit Advanced Analog Flash Microcontroller*. Retrieved from <http://ww1.microchip.com/downloads/en/DeviceDoc/40001579E.pdf>

Powers, N., Alling, A., Gyampoh-Vidogah, R., & Soyata, T. (2014). AXaaS: Case for Acceleration as a Service. *IEEE Globecom 2014 Workshop on Cloud Computing Systems, Networks, and Applications*.

Prasad, K., Sharma, V., Lackore, S. M., Jenkins, K., Prasad, A., & Sood, A. (2013). *The American Journal of Cardiology*, 339-345.

Quwaider, M., & Jararweh, Y. (2013). Cloudlet-based for big data collection in body area networks. *International Conference for Internet Technology and Secured Transactions (ICITST)*, (pp. 137-141).

Rao, B., Saluia, P., Sharma, N., Mittal, A., & Sharma, S. (2012). Cloud computing for internet of things sensing based applications. *Sixth International Conference on Sensing Technology (ICST)*, (pp. 374-380).

Salamifar, S. E., & Lai, R. Y. (2013). Use of combined scanning electrochemical and fluorescence microscopy for detection of reactive oxygen species in prostate cancer cells. *Analytical chemistry*, 9417-9421.

Satyanarayanan, M., Bahl, P., Caceres, R., & Davies, N. (2009). The case for vm-based cloudlets in mobile computing. *Pervasive Computing*, 14-23.

Saul, J., Schwartz, P. J., Ackerman, P. J., & Triedman, J. K. (2014). Rationale and objectives for ECG screening in infancy. *Heart rhythm : the official journal of the Heart Rhythm Society*, 2316-2321.

Searles, C. D. (2002). The nitric oxide pathway and oxidative stress in heart failure. *Congestive Heart Failure*, 142-155.

Sensys Medical, I. (n.d.). *Near-Infrared Spectroscopy*. Retrieved from <http://www.diabetesnet.com/diabetes-technology/meters-monitors/future-meters-monitors/sensys-medical>

- Shah, R. (2004). Drug-induced QT interval prolongation: regulatory perspectives and drug development. *Annals of medicine*, 36, 47-52.
- Shahabi, C. (2013). Towards a generic framework for trustworthy spatial crowdsourcing. *12th International ACM Workshop on Data Engineering for Wireless and Mobile Access (MobiDE)*, (pp. 1-4).
- Sharpe, E., Bradley, R., Frasco, T., Jayathilaka, D., Marsh, A., & Andreescu, S. (2014). Metal oxide based multisensor array and portable database for field analysis of antioxidants. *Sensors and Actuators B: Chemical*, 552-562.
- Sharpe, E., Frasco, T., Andreescu, D., & Andreescu, S. (2013). Portable ceria nanoparticle-based assay for rapid detection of food antioxidants (nanocerac). *Analyst*, 249-262.
- Sheng, X., Tang, J., Xiao, X., & Xue, G. (2013). Sensing as a service: Challenges, solutions and future directions. *IEEE Sensors Journal*, 3733-3741.
- Shoukry, Y., Martin, P., Tabuada, P., & Srivastava, M. (2013). Non-invasive spoofing attacks for anti-lock braking systems. In G. Bertoni, & J. S. Coron, *Cryptographic Hardware and Embedded Systems* (pp. 55-72). Heidelberg, Germany: Springer.
- Singh, N. (1995). Oxidative stress and heart failure. 77-81.
- Sorenson, H. W. (1970, July). Least-squares estimation: from Gauss to Kalman. *IEEE Spectrum*, pp. 63-68.
- Soyata, T., Ba, H., Heinzelman, W., Kwon, M., & Shi, J. (2013). Accelerating mobile cloud computing: A survey. In *Communication Infrastructures for Cloud Computing* (pp. 175-197). Hershey, Pennsylvania: IGI Global.
- Soyata, T., Friedman, E. G., & Mulligan, J. H. (1997, January). Incorporating Interconnect, Register, and Clock Distribution Delays into the Retiming Process. *IEEE Transactions on Computer Aided Design of Integrated Circuits and Systems*, 16(1), 105-120.
- Soyata, T., Muraleedharan, R., Ames, S., Langdon, J., Funai, C., Kwon, M., & Heinzelman, W. (2012). COMBAT: mobile Cloud-based cOmpute/coMmunications infrastructure for BATtlefield applications. *Proceedings of SPIE*, 8403, pp. 84030K-84030K. Baltimore, MD.
- Soyata, T., Muraleedharan, R., Funai, C., Kwon, M., & Heinzelman, W. (2012). Cloud-Vision: Real-time face recognition using a mobile-cloudlet-cloud acceleration architecture. *Computers and Communications (ISCC), 2012 IEEE Symposium on*, 59-66.
- SQLite. (2015). Retrieved from <https://www.sqlite.org/>
- Stramba-Badiale, M., Priori, S. G., Napolitano, C., Locati, E. H., Vinolas, X., Haverkamp, W., . . . Schwartz, P. J. (2000). Gene-specific differences in the circadian variation of ventricular repolarization in the long QT syndrome: a key to sudden death during sleep? *Ital Heart J*, 323-328.

- Sun, Y., Luo, H., & Das, S. (2012). A trust-based framework for fault-tolerant data aggregation in wireless multimedia sensor networks. *IEEE Transactions on Dependable and Secure Computing*, 785-797.
- Tsutsui, H. (2001). Oxidative stress in heart failure: the role of mitochondria. *Internal medicine (Tokyo, Japan)*, 1177-1182.
- Vatta, M. (2009). Intronic variants and splicing errors in cardiovascular diseases. *Heart rhythm : the official journal of the Heart Rhythm Society*, 219-220.
- Vazquez, J., & Ipina, D. L. (2008). Social devices: Autonomous artifacts that communicate on the internet. In *The Internet of Things* (pp. 308-324). Berlin, Germany: Springer-Verlag.
- Wang, H., Liu, W., & Soyata, T. (2014). Accessing Big Data in the Cloud Using Mobile Devices. In P. R. Dek, *Handbook of Research on Cloud Infrastructures for Big Data Analytics* (pp. 444-470). Hershey, Pennsylvania: IGI Global. doi:10.4018/978-1-4666-5864-6.ch018
- Winterbourn, C. C. (2008). Reconciling the chemistry and biology of reactive oxygen species. *Nature chemical biology*, 278-286.
- Wojciechowska, C., Romuk, E., Tomasiak, A., Skrzep-Poloczek, B., Nowalany-Kozielska, E., Birkner, E., & Jachec, W. (2014). Oxidative stress markers and c-reactive protein are related to severity of heart failure in patients with dilated cardiomyopathy. *Mediators of Inflammation*.
- Zhang, W., Das, S., & Liu, Y. (2006). A trust based framework for secure data aggregation in wireless sensor networks. *3rd Annual IEEE Communications Society on Sensor and Ad Hoc Communications and Networks*, (pp. 60-69).
- Zhang, Y., Meratnia, N., & Havinga, P. (2010). Outlier detection techniques for wireless sensor networks: A Survey. *IEEE Communications Surveys Tutorials*, 159-170.